

The Multi-cluster Two-Wave Fading Model

Juan P. Peña-Martín, Maryam Olyaei, F. J. Lopez-Martinez and Juan M. Romero-Jerez

Abstract—We introduce and characterize a natural generalization of Durgin’s Two-Wave with Diffuse Power (TWDP) fading model, by allowing that the incident waves arrive in different clusters. The newly proposed model, referred to as the Multi-cluster Two-Wave (MTW) fading model, generalizes *both* the TWDP and the κ - μ models under a common umbrella. The special case on which the model parameters reach extreme values is also analyzed, aimed to model harsh fading conditions reported in experimental measurements obtained in enclosed environments. The chief probability functions of both the MTW and the MTW Extreme fading models are obtained, including the probability density function, the cumulative distribution function and the generalized moment-generating function. A number of applications for these models are exemplified, including outage probability in interference-limited scenarios, energy detection, and composite fading modeling.

Index Terms—Multicenter, Fading, Generalized Moment Generating Function, Energy Detection, Outage Probability, Composite Fading.

I. INTRODUCTION

The new use cases defined for 5G/6G wireless cellular communications systems, as well as the use of new spectral bands, including millimeter-wave (mmWave) and terahertz radio signals, give rise to new propagation scenarios not considered until now. Also, the massive deployment of wireless sensor networks involve some extreme environments, including underwater, underground, enclosed or harsh industrial scenarios (e.g., shipping containers, oil/gas pipelines and platforms, etc.) where the propagation conditions largely differ from the assumptions considered in the derivation of traditional stochastic wireless models. Therefore, new statistical wireless fading models are necessary for the design, planning and performance evaluation of the foreseen wireless networks.

Rice (or Rician) fading has been traditionally used to model line-of-sight propagation scenarios, as it consists of a single cluster of waves, made up of a multitude of weakly scattered components, plus an additional constant-amplitude specular (dominant) wave with arbitrary power. The Rice fading model

has been generalized in a number of ways in the literature: for instance, the κ - μ fading model was originally proposed in [2] and considers a signal composed of μ clusters of waves each of which may contain a specular component as in the Rice model. Within any cluster, the phases of the waves are random and have very small (negligible, in practice) delay times, while the delay times among the different clusters show greater differences, in such a way that each cluster can independently be resolved and combined at the receiver, i.e., this physical description of the κ - μ fading implies that it can be used to model frequency-selective wireless channels. The number of clusters μ should be, in principle, a positive integer; however, a better fit to experimental data is facilitated if μ is allowed to take any positive real value [3]. It must be remarked that the mathematical description of the κ - μ model is a function, among other factors, of the total aggregate power of the specular components, but it is oblivious to the power of the individual specular components and how many clusters incorporate them.

On the other hand, the Two-Wave with Diffuse Power (TWDP) fading model was originally proposed in [4] and provides an alternative generalization of the Rice model. It considers two specular components with random phases plus a diffuse component, representing a single cluster of multiple scattered waves. This model includes a wide variety of propagation conditions ranging from very favorable to worse than Rayleigh fading (hyper-Rayleigh fading) [5]. The TWDP fading model has been used to model propagation conditions in the mmWave band, and has been shown to provide a better match than the Rice fading in indoor wireless channels at 60 GHz [6].

In this work, we introduce a Multi-cluster Two-Wave (MTW) fading model, which generalizes the Rice fading in two ways: by considering *both* multiple clusters of waves (in a κ - μ fashion), and also by allowing more than one specular component within one of the given clusters (in a TWDP fashion). Specifically, the MTW fading model consists of an arbitrary number of wave clusters, where the first received cluster incorporates two specular components: one typically resulting from a direct link between transmitter and receiver and another from a strong reflection. The remaining clusters are assumed to reach the receiver from multiple reflections and are therefore composed of a number of scattered waves in which a specular component may also be present. This model has physical meaning in rich scattering environments, giving rise to many propagation paths, with a line-of sight in the transmitter-receiver link, resulting in the aforementioned two dominant components in the first received cluster.

It is worth noting that the proposed MTW fading model unifies both the κ - μ and TWDP models in the same mathematical framework. Encapsulating such relevant models, that

The authors are with Communications and Signal Processing Lab, Instituto Universitario de Investigación en Telecomunicación (TELMA), Universidad de Málaga, CEI Andalucía TECH. ETSI Telecomunicación, Bulevar Louis Pasteur 35, 29010 Málaga, Spain. F.J. López-Martínez is also with the Department of Signal Theory, Networking and Communications, Universidad de Granada, 18071, Granada, Spain. (e-mails: jppena@uma.es, olyaei@uma.es, fjlopezm@ugr.es, romero@dte.uma.es).

This work was presented in part at the 2022 5th International Conference on Advanced Communication Technologies and Networking (CommNet) [1].

This work was funded in part by Junta de Andalucía and the European Fund for Regional Development FEDER through projects P21-00420 and P18-RT-3175, in part by “Consejería de Transformación Económica, Industria, Conocimiento y Universidades” within the talent acquisition program EMERGIA (ref. EMERGIA20_00297), and in part by MCIN/AEI/10.13039/501100011033 through grant PID2020-118139RB-I00.

This work has been submitted to the IEEE for publication. Copyright may be transferred without notice, after which this version may no longer be accessible.

have already been extensively empirically validated by field measurement campaigns, in the same formulation is another key novel contribution of this work. This permits to integrate many results previously obtained for the aforementioned models, which have been studied up until now separately and whose results are scattered throughout the technical literature. Moreover, the proposed MTW model is more general than the κ - μ and the TWDP models alone, and expands to other possible wireless environments not included in any of them when considered separately. Strikingly, this generalization does not come at the prize of an increased mathematical complexity.

To further demonstrate its flexibility, and inspired by the κ - μ Extreme distribution [3], [7], we additionally introduce and characterize the MTW Extreme distribution, which is obtained when the MTW model parameters μ and K reach their extreme values, i.e. $\mu \rightarrow 0$ and $K \rightarrow \infty$, for a given fading severity quantified by the Amount of Fading, i.e. keeping $K\mu$ constant. These extreme distributions find applicability in very severe fading conditions such as enclosed environments, namely tunnels, shipping containers (which could host wireless sensors) and public transportation vehicles, including airplanes, trains, and buses. In these and other extreme environments, the Central Limit Theorem (which classical statistical fading models generally assume) may not hold due to the low number of radio paths. In some cases, severe channel variations may result in a non-negligible probability that the received signal is below the receiver sensitivity [7], resulting in null reception. This feature is also captured by the MTW Extreme distribution, rendering a versatile and general model for extreme environments propagation. In other instances, the Two-Ray fading model [5] is also a good candidate to model these harsh propagation conditions. Noteworthy, the Two-Ray model is also a particular case of the proposed MTW Extreme model, so that a wider set of propagation conditions can be captured by this model.

We derive easy-to-compute exact expressions for the probability density function (PDF) and the cumulative distribution function (CDF) of the received signal-to-noise ratio (SNR) under MTW and MTW Extreme fading. Additionally, the generalized moment generating function (GMGF) of both models is given in closed-form, which allows to obtain many different performance metrics of wireless communications systems undergoing the new proposed models. In particular, closed-form expressions are obtained for the outage probability in interference-limited and noise-limited scenarios, and for the energy detection probability. We also exemplify how the MTW model can be further generalized to include the effect of shadowing, in a straightforward way [8].

The rest of this paper is organized as follows: In Section II, the MTW channel model is presented, and the PDF, CDF, and generalized MGF are derived. These statistical functions are also derived for the MTW Extreme fading in Section III. In Section IV, different performance metrics for the proposed models are presented, including the outage probabilities, energy detection and composite fading modeling. Numerical results are given in Section V, followed by the concluding remarks in Section VI.

II. MTW CHANNEL MODEL

The Multi-cluster Two-Wave fading model results from the combination of multiple signal clusters, being one of them, typically the first one received, accompanied by two specular components representing dominant waves, while the remaining clusters may include one specular component. Let us assume that μ signal clusters are received. The complex baseband signal amplitude of the first cluster can be expressed as

$$Z_1 = V_{1,1} \exp(j\phi_{1,1}) + V_{1,2} \exp(j\phi_{1,2}) + X_1 + jY_1, \quad (1)$$

while for the other $(\mu - 1)$ clusters we have,

$$Z_i = V_i \exp(j\phi_i) + X_i + jY_i, \quad i = 2, \dots, \mu, \quad (2)$$

where $V_{1,k}$ and $\phi_{1,k}$ indicate, respectively, the k -th specular component ($k = 1, 2$) amplitude and uniformly distributed random phase in the interval $[0, 2\pi)$, $\phi_{1,k} \sim \mathcal{U}[0, 2\pi)$, of the first cluster; while V_i and ϕ_i indicate, respectively, the specular component amplitude and phase, $\phi_i \sim \mathcal{U}[0, 2\pi)$, of the i -th cluster, ($i = 2, \dots, \mu$). On the other hand, $(X_n + jY_n)$, ($n = 1, \dots, \mu$), are complex Gaussian random variables (RVs) with $X_n, Y_n \sim \mathcal{N}(0, \sigma^2)$, representing the contributions due to the combined reception of numerous weak scattered waves.

In the MTW fading model, the delay-time spreads of the different clusters are assumed to be relatively large, and the received power is a result of the summation of the different clusters powers. Thus, we can write $W = R^2 = \sum_{i=1}^{\mu} |Z_i|^2$, where W and R represent the received power and signal envelope, respectively.

A. Probability distribution (PDF and CDF)

In the following, the PDF of the SNR of the MTW fading model is derived. Let us define the following two random variables:

$$\begin{aligned} \theta &\triangleq \phi_{1,1} - \phi_{1,2} \\ d_\theta^2 &\triangleq (V_{1,1} \cos \phi_{1,1} + V_{1,2} \cos \phi_{1,2})^2 \\ &\quad + (V_{1,1} \sin \phi_{1,1} + V_{1,2} \sin \phi_{1,2})^2 + \sum_{i=2}^{\mu} V_i^2 \\ &= V_{1,1}^2 + V_{1,2}^2 + 2V_{1,1}V_{1,2} \cos \theta + \sum_{i=2}^{\mu} V_i^2. \end{aligned} \quad (3)$$

Note that d_θ^2 represents the total power of the specular components in terms of the RV θ , which follows a triangular distribution in the interval $[-2\pi, 2\pi)$, and which is equivalent to a uniform distribution in $[0, 2\pi)$ due to the 2π periodicity of the phases.

The signal complex amplitude of the first cluster given in (1) can be rewritten in terms of θ as

$$Z_1 = e^{j\phi_{1,2}} (V_{1,1} e^{j\theta} + V_{1,2}) + X_1 + jY_1. \quad (4)$$

Thus, for a given particular realization of variable θ , (4) is equivalent to the signal of a cluster with a single specular component with amplitude $|V_{1,1} \exp(j\theta) + V_{1,2}|$. Thus, the set of clusters forms a κ - μ channel as in [3] when conditioned on

θ . Hence, the conditional PDF of the received signal power for a given θ , W_θ , will be expressed as

$$f_{W|\theta}(w) = \frac{1}{2\sigma^2} \left(\frac{w}{d_\theta^2} \right)^{\frac{\mu-1}{2}} \exp\left(-\frac{w}{2\sigma^2} - \frac{d_\theta^2}{2\sigma^2}\right) \times I_{\mu-1}\left(\sqrt{w} \frac{d_\theta}{\sigma^2}\right), \quad (5)$$

where I_ν is the modified Bessel function of the first kind with order ν . Introducing the parameter

$$\kappa_\theta \triangleq \frac{d_\theta^2}{2\sigma^2\mu}, \quad (6)$$

which represents the ratio between the specular components power, conditioned on θ , and the total average diffuse power from all the clusters, we can write the average conditioned power as

$$\overline{W}_\theta = d_\theta^2 + 2\sigma^2\mu = 2\sigma^2\mu(1 + \kappa_\theta). \quad (7)$$

Thus, by combining (6) and (7), we can write,

$$d_\theta^2 = \frac{\overline{W}_\theta}{(1 + \kappa_\theta)} \kappa_\theta. \quad (8)$$

Let us now introduce the random variable $\gamma \triangleq WE_s/N_0$ representing the received SNR, where E_s is the symbol energy and N_0 is the one-sided AWGN power spectral density. Thus, denoting by $\overline{\gamma}_\theta$ the conditioned, on θ , average SNR, we have that $E_s/N_0 = \frac{\overline{\gamma}_\theta}{\overline{W}_\theta}$, and

$$\gamma_{|\theta} = W_\theta \frac{\overline{\gamma}_\theta}{\overline{W}_\theta}. \quad (9)$$

Thus, from (5) and considering (9), the PDF of the conditioned SNR will be

$$f_{\gamma|\theta}(x) = \frac{\overline{W}_\theta}{\overline{\gamma}_\theta} f_{W|\theta}\left(\frac{\overline{W}_\theta}{\overline{\gamma}_\theta} x\right) = \frac{\mu(1 + \kappa_\theta)^{\frac{\mu+1}{2}}}{\overline{\gamma}_\theta e^{\mu\kappa_\theta}} \left(\frac{x}{\overline{\gamma}_\theta \kappa_\theta}\right)^{\frac{\mu-1}{2}} e^{-\frac{\mu(1+\kappa_\theta)}{\overline{\gamma}_\theta} x} \times I_{\mu-1}\left(2\mu\sqrt{\frac{\kappa_\theta(1 + \kappa_\theta)}{\overline{\gamma}_\theta}} x\right). \quad (10)$$

As the expected unconditional power is $\overline{W} = V_{1,1}^2 + V_{1,2}^2 + \sum_{i=2}^{\mu} V_i^2 + 2\sigma^2\mu$ and $E_s/N_0 = \frac{\overline{\gamma}_\theta}{\overline{W}_\theta} = \frac{\overline{\gamma}}{\overline{W}}$, we can write

$$\begin{aligned} \overline{\gamma}_\theta &= \overline{\gamma} \frac{\overline{W}_\theta}{\overline{W}} \\ &= \overline{\gamma} \frac{V_{1,1}^2 + V_{1,2}^2 + 2V_{1,1}V_{1,2} \cos \theta + \sum_{i=2}^{\mu} V_i^2 + 2\sigma^2\mu}{V_{1,1}^2 + V_{1,2}^2 + \sum_{i=2}^{\mu} V_i^2 + 2\sigma^2\mu} \\ &= \overline{\gamma} \left(1 + \frac{2V_{1,1}V_{1,2} \cos \theta}{V_{1,1}^2 + V_{1,2}^2 + \sum_{i=2}^{\mu} V_i^2 + 2\sigma^2\mu} \right), \end{aligned} \quad (11)$$

The MTW fading model can be conveniently described in terms of parameters K and Δ , defined as

$$K \triangleq \frac{V_{1,1}^2 + V_{1,2}^2 + \sum_{i=2}^{\mu} V_i^2}{2\sigma^2\mu}, \quad (12)$$

$$\Delta \triangleq \frac{2V_{1,1}V_{1,2}}{V_{1,1}^2 + V_{1,2}^2 + \sum_{i=2}^{\mu} V_i^2},$$

where K represents the ratio between the average power of the specular components and the diffuse components power from all the clusters; and $\Delta + 1$ is the peak-to-average ratio of specular powers, verifying $0 \leq \Delta \leq P_1/(P_1 + P_0) \leq 1$ with $P_1 \triangleq V_{1,1}^2 + V_{1,2}^2$ and $P_0 \triangleq \sum_{i=2}^{\mu} V_i^2$ denoting, respectively, the average specular power of the first cluster and the specular power of the rest of the clusters. The more similar the amplitude of the specular components of the first cluster the higher the value of Δ , while $\Delta = 0$ is attained when only one specular component is present in the first cluster. When all the specular power is concentrated in the first cluster, or it is the only one received, then $\Delta = 1$ can be reached, indicating that both specular components have the same amplitude.

After some manipulations, (11) can be written in terms of parameters K and Δ as

$$\overline{\gamma}_\theta = \overline{\gamma} \frac{1 + K(1 + \Delta \cos \theta)}{1 + K}, \quad (13)$$

and with the help of (6) and (3) we can write

$$\kappa_\theta = K(1 + \Delta \cos \theta). \quad (14)$$

Therefore, from (13) and (14) we can conclude that

$$\frac{1 + \kappa_\theta}{\overline{\gamma}_\theta} = \frac{1 + K(1 + \Delta \cos \theta)}{\overline{\gamma} \frac{1 + K(1 + \Delta \cos \theta)}{1 + K}} = \frac{1 + K}{\overline{\gamma}}, \quad (15)$$

which shows that the ratio $(1 + \kappa_\theta)/\overline{\gamma}_\theta$ is invariant with respect to θ . Substituting (13), (14) and (15) into (10), the conditional PDF of the SNR becomes

$$f_{\gamma|\theta}(x) = \frac{\mu(1 + K)^{\frac{\mu+1}{2}}}{\overline{\gamma} e^{\mu\kappa_\theta}} \left(\frac{x}{\overline{\gamma} \kappa_\theta}\right)^{\frac{\mu-1}{2}} \times e^{-\frac{\mu(1+K)}{\overline{\gamma}} x} I_{\mu-1}\left(2\mu\sqrt{\frac{\kappa_\theta(1 + K)}{\overline{\gamma}}} x\right). \quad (16)$$

The unconditional PDF of the SNR γ can be obtained by averaging over the realizations of the RV θ , which yields the result given in the following lemma.

Lemma 1: Let γ represent the received SNR in an MTW fading channel. Then, the PDF of γ is given by

$$f_\gamma(x) = \frac{\mu}{\pi} \left(\frac{1 + K}{\overline{\gamma}}\right)^{\frac{\mu+1}{2}} e^{-\mu K} \left(\frac{x}{\overline{\gamma}}\right)^{\frac{\mu-1}{2}} e^{-\mu \frac{1+K}{\overline{\gamma}} x} \times \int_0^\pi e^{-\mu K \Delta \cos \theta} (1 + \Delta \cos \theta)^{\frac{1-\mu}{2}} \times I_{\mu-1}\left(2\mu\sqrt{\frac{1 + K}{\overline{\gamma}}} K(1 + \Delta \cos \theta)x\right) d\theta. \quad (17)$$

Proof: Taking into account that $\cos \theta$ is symmetric around π , and the fact that the PDF of θ is $f_\theta(\theta) = \frac{1}{2\pi}$, constant in the interval $[0, 2\pi)$, (17) is obtained by considering (14) and averaging (16) with respect to θ . ■

Although (17) is not strictly a closed-form expression, it is given in terms of a definite integration of a smooth integrand. Therefore, its numerical computation is straightforward, similarly to the case of TWDP fading [9]. For $\mu = 1$, the MTW model collapses to the TWDP one, and (17) is equivalent to [9, eq. (26)]. On the other hand, if $\Delta = 0$, (17) is equivalent to [3, eq. (2)] and we obtain the κ - μ channel model (note that in this case the integration is trivial and can be solved in closed-form). To the best of our knowledge, no other previously proposed statistical fading model contains such different models such as κ - μ and TWDP as special cases, which gives a great versatility to the MTW fading model. Note also that both models have been used independently to fit different wireless environments, thus justifying the validity of the general MTW model, as it encompasses both of them as special cases.

Corollary 1: The CDF of the received SNR γ in an MTW fading channel is given by

$$F_\gamma(x) = 1 - \frac{1}{\pi} \int_0^\pi Q_\nu \left(\sqrt{2\mu K(1 + \Delta \cos \theta)}, \sqrt{2x\mu\zeta} \right) d\theta, \quad (18)$$

with $\zeta \triangleq \frac{1+K}{\bar{\gamma}}$ and where $Q_\nu(a, b)$ is the ν -th order generalized Marcum Q -function as defined as [10, eq. (4.60)]

$$Q_\nu(a, b) = a^{1-\nu} \int_b^\infty x^\nu \exp \left[-\frac{x^2 + a^2}{2} \right] I_{\nu-1}(ax) dx. \quad (19)$$

Proof: Considering

$$F_\gamma(x) = \int_0^x f_\gamma(t) dt = 1 - \int_x^\infty f_\gamma(t) dt, \quad (20)$$

and introducing (17) into (20), the result given in (18) is obtained, after some manipulation, by changing the integration order of variables θ and t and performing the transformation $t = \frac{z^2}{2\mu\zeta}$. ■

B. Generalized moment generating function

The generalized MGF of the SNR is defined as [11]

$$\phi_\gamma^{(n)}(s) \triangleq E \{ \gamma^n e^{\gamma s} \} = \int_0^\infty x^n e^{xs} f_\gamma(x) dx, \quad (21)$$

where $E \{ \cdot \}$ denotes the expectation operator. In the sequel, we will assume $n \in \mathbb{N}$. In this case, the generalized MGF coincides with the n -th order derivative of the MGF.

Lemma 2: Let γ represent the received SNR in an MTW fading channel. Then, the generalized MGF of γ , $\phi_\gamma^{(n)}(s)$, is given by (22).

Proof: See Appendix A. ■

Unlike the PDF or the CDF, the generalized MGF of the SNR under the MTW fading channel has a closed-form expression in terms of a finite number of well-known functions. This enables an exact analysis of different performance metrics without increasing the analytical complexity when compared to simpler cases, such as for TWDP or κ - μ fading.

Corollary 2: The MGF of the SNR γ in an MTW fading channel is given by

$$M_\gamma(s) = \left(\frac{\mu(1+K)}{\mu(1+K) - \bar{\gamma}s} \right)^\mu \times \exp \left(\frac{\mu K \bar{\gamma} s}{\mu(1+K) - \bar{\gamma}s} \right) I_0 \left(\frac{\mu K \Delta \bar{\gamma} s}{\mu(1+K) - \bar{\gamma}s} \right). \quad (23)$$

Proof: The MGF is defined as $M_\gamma(s) \triangleq E \{ e^{\gamma s} \} = \phi_\gamma^{(0)}(s)$. Thus, substituting $n = 0$ in (22), (23) is obtained. ■

Corollary 3: The n -th order non-central moment of the SNR γ is given by

$$\nu_n = \left(\frac{\bar{\gamma}}{\mu(1+K)} \right)^n \Gamma(\mu+n) \sum_{q=0}^n \binom{n}{q} \frac{(\mu K)^q}{\Gamma(\mu+q)} \times \sum_{r=0}^q \binom{q}{r} \left(\frac{\Delta}{2} \right)^r \sum_{l=0}^r \binom{r}{l} \delta_{2l,r}, \quad (24)$$

where $\delta_{2l,m}$ is the kronecker delta function.

Proof: The proof follows from (22) by considering that $\nu_n = \phi_\gamma^{(n)}(0)$ and noting that $I_0(0) = 1$ and $I_\nu(0) = 0$ for $\nu \neq 0$. ■

It is easy to check that $\nu_0 = 1$ and $\nu_1 = \bar{\gamma}$, as expected.

The amount of fading (AoF) is a fading metric introduced in [12] as the SNR variance normalized to its squared mean, i.e.,

$$\text{AoF} = \frac{\text{Var}(\gamma)}{(E[\gamma])^2} = \frac{\nu_2 - \bar{\gamma}^2}{\bar{\gamma}^2}. \quad (25)$$

The AoF for the MTW can be calculated as stated in the next corollary.

Corollary 4: The AoF in an MTW fading channel is given by

$$\text{AoF} = \frac{1}{(1+K)^2} \left[\frac{1+2K}{\mu} + \frac{K^2 \Delta^2}{2} \right]. \quad (26)$$

Proof: The proof follows from (24) and (25) by simple substitution. ■

In the literature, it is frequent to use the fading parameter $m = 1/\text{AoF}$, by similarity to the Nakagami- m fading parameter, as the AoF of this latter model is, precisely, $1/m$.

C. Asymptotic CDF and diversity order

An asymptotic expression of the CDF in the high SNR regime is useful to obtain insight of the effect of system parameters on performance, as the CDF is closely related to the outage probability, as we will later show. To obtain such expression we first note that, by taking the limit $s \rightarrow \infty$ in the MGF given in (23), the following expression holds:

$$|M_\gamma(s)| = \frac{\mu^\mu (1+K)^\mu}{e^{\mu K}} I_0(\mu K \Delta) \frac{1}{\bar{\gamma}^\mu |s|^\mu} + o(|s|^{-\mu}). \quad (27)$$

Then, from Propositions 3 and 5 in [13] the asymptotic CDF can be expressed as

$$F_\gamma(x) = \frac{\mu^\mu (1+K)^\mu}{\Gamma(\mu+1) e^{\mu K}} I_0(\mu K \Delta) \left(\frac{x}{\bar{\gamma}} \right)^\mu + o(\bar{\gamma}^{-\mu}). \quad (28)$$

It is clear from (28) that the diversity order of the MTW model is μ .

$$\begin{aligned} \phi_{\gamma}^{(n)}(s) &= \bar{\gamma}^n \Gamma(\mu + n) \exp\left(\frac{\mu K \bar{\gamma} s}{\mu(1+K) - \bar{\gamma} s}\right) \sum_{q=0}^n \binom{n}{q} \frac{(\mu K)^q}{\Gamma(\mu + q)} \frac{(\mu(1+K))^{\mu+q}}{(\mu(1+K) - \bar{\gamma} s)^{\mu+q+n}} \\ &\times \sum_{r=0}^q \binom{q}{r} \left(\frac{\Delta}{2}\right)^r \sum_{l=0}^r \binom{r}{l} I_{2l-r}\left(\frac{\mu K \Delta \bar{\gamma} s}{\mu(1+K) - \bar{\gamma} s}\right). \end{aligned} \quad (22)$$

III. MTW EXTREME DISTRIBUTION

The MTW Extreme distribution is derived from the MTW distribution for the case when $K \rightarrow \infty$ (very strong dominant components) and $\mu \rightarrow 0$ (almost no multipath clustering), while the product $K\mu$ remains constant, which results in the AoF being fixed.

A. Probability distribution (PDF and CDF)

From the AoF of the MTW fading (26), and considering the parameter values defined for the MTW Extreme distribution, the AoF (i.e., $1/m$) will be given in this case by

$$\frac{1}{m} = \frac{2}{K\mu} + \frac{\Delta^2}{2}. \quad (29)$$

Note that for the κ - μ Extreme distribution, equality $\kappa\mu = 2m$ holds [7], which is actually the result in (29) for $\Delta = 0$ (single specular component). Note also that the model parameters m and Δ are related, as the more balanced the specular components of the first cluster (Δ closer to 1), the more severe the fading (lower m and higher AoF). This is due to the fact that, the higher the value of Δ the more similar are the specular components, and therefore the higher is the probability that the specular components cancel each other, yielding to deep signal fades.

For the sake of compactness, in the subsequent mathematical expressions of the MTW Extreme model, instead of m , the following parameter will be used

$$\xi \triangleq K\mu = \frac{2m}{1 - m\frac{\Delta^2}{2}}. \quad (30)$$

Note that for the parameters to make physical sense (i.e., in order to avoid the singularity and negative values for the product $K\mu$) the condition $m < \frac{2}{\Delta^2}$ must be satisfied.

Lemma 3: The CDF of the SNR γ in an MTW Extreme fading channel is given by

$$\begin{aligned} F_{\gamma E}(x) &= u(r) \left[1 - \frac{1}{\pi} \right. \\ &\times \left. \int_0^{\pi} Q_0\left(\sqrt{2\xi(1 + \Delta \cos \theta)}, \sqrt{\frac{2x\xi}{\bar{\gamma}}}\right) d\theta \right]. \end{aligned} \quad (31)$$

Proof: The proof follows by applying the extreme conditions ($K\mu = \xi$ being a constant, with $K \rightarrow \infty$ and $\mu \rightarrow 0$) to (18). ■

Note that the Heaviside step function $u(r)$ is always implicit in the distributions of non-negative variables, but it is not necessary to make it explicit when the function is continuous at 0, which is not the case here as there is a certain probability, given by $F_{\gamma E}(0)$, that no signal is received.

Corollary 5: The PDF of the SNR γ in an MTW Extreme fading channel is given by

$$\begin{aligned} f_{\gamma E}(x) &= \frac{\xi}{\pi\sqrt{x\bar{\gamma}}} \exp\left[-\xi\left(1 + \frac{x}{\bar{\gamma}}\right)\right] \\ &\times \int_0^{\pi} \sqrt{1 + \Delta \cos \theta} \exp[-\xi\Delta \cos \theta] \\ &I_1\left(2\xi\sqrt{x\frac{1 + \Delta \cos \theta}{\bar{\gamma}}}\right) d\theta + C\delta(x), \end{aligned} \quad (32)$$

with $C = e^{-\xi} I_0(\xi\Delta)$ and where $\delta(\cdot)$ is the Dirac delta function.

Proof: The PDF is obtained by applying the extreme conditions ($K \rightarrow \infty$, $\mu \rightarrow 0$ and $K\mu = \xi$) to (17) or, equivalently, as the derivative of (31). However, care must be taken when considering limit values in the parameters of a probability distribution as a discontinuity may appear in the CDF. This is precisely our case, where there is a discontinuity at the origin of the CDF that will yield the appearance of a Dirac Delta function at the origin of the PDF. For a PDF to be valid, it must verify $\int_0^{\infty} f_{RE}(r) dr = 1$. As the derivative of the step function is a Dirac Delta function, this function appears in the PDF expression with a weight factor C in order to meet the aforementioned requirement. Again, this means a non-zero probability that a null signal is measured, that is, the received power is below the detection limits of the receiver. It is clear that $C = F_{RE}(0^+)$.

The expression of C can be obtained by considering the extreme conditions ($K \rightarrow \infty$, $\mu \rightarrow 0$ and $K\mu = \xi$) in (28), as this equation is the asymptotic behavior of the CDF of the SNR at the origin, yielding

$$C = e^{-\xi} I_0(\xi\Delta). \quad (33)$$

B. Generalized moment generating function

We now obtain a closed-form expression for the GMGF of the SNR in an MTW Extreme channel.

Corollary 6: The GMGF of the SNR γ in an MTW Extreme fading channel is given by (34).

Proof: This result is obtained by applying the extreme conditions to (22), ■

Corollary 7: The MGF of the SNR γ in an MTW Extreme fading channel is given by

$$M_{\gamma E}(s) = \exp\left(\frac{\xi \bar{\gamma} s}{\xi - \bar{\gamma} s}\right) I_0\left(\frac{\xi \Delta \bar{\gamma} s}{\xi - \bar{\gamma} s}\right). \quad (35)$$

$$\phi_\gamma^{(n)}(s) = \bar{\gamma}^n \Gamma(n) \exp\left(\frac{\xi \bar{\gamma} s}{\xi - \bar{\gamma} s}\right) \sum_{q=0}^n \binom{n}{q} \frac{1}{\Gamma(q)} \frac{\xi^{2q}}{(\xi - \bar{\gamma} s)^{n+q}} \sum_{r=0}^q \binom{q}{r} \left(\frac{\Delta}{2}\right)^r \sum_{l=0}^r \binom{r}{l} I_{2l-r}\left(\frac{\xi \Delta \bar{\gamma} s}{\xi - \bar{\gamma} s}\right). \quad (34)$$

Proof: This result can be obtained by applying the extreme conditions to (23) or, equivalently, by setting $n = 0$ in (34). ■

Corollary 8: The n -th order non-central moment of the SNR γ in an MTW Extreme fading channel is given by

$$\begin{aligned} \nu_n &= \left(\frac{\bar{\gamma}}{\xi}\right)^n \Gamma(n) \sum_{q=0}^n \binom{n}{q} \frac{\xi^q}{\Gamma(q)} \\ &\times \sum_{r=0}^q \binom{q}{r} \left(\frac{\Delta}{2}\right)^r \sum_{l=0}^r \binom{r}{l} \delta_{2l,r}. \end{aligned} \quad (36)$$

Proof: This result is obtained by applying the extreme conditions to (24) or, equivalently, by setting $s = 0$ in (34). ■

C. Two-Ray fading model

The Two-Ray fading model was proposed in [5] for severe fading conditions, providing in some cases even better fitting results than the κ - μ Extreme model [7]. The Two-Ray fading model (with hyper-Rayleigh behavior) consists of two waves of approximately the same amplitude (so that they can become completely deconstructive) without diffuse component; therefore, it can be obtained from the MTW distribution by setting $\Delta \approx 1$, and letting $K \rightarrow \infty$ and any positive real value of μ . Therefore, this model can also be obtained from the MTW Extreme distribution for $\Delta = 1$ and $m = 2$, with both conditions implying $\xi \rightarrow \infty$. The MGF of an N -Ray model with arbitrary powers was given in [14, eq. (17)], from which the MGF for the Two-Ray model can be obtained. The GMGF and non-central moments of the Two-Ray model can be expressed in closed-form as shown in the following corollary, where the MGF is also provided for the sake of completeness.

Corollary 9: The GMGF, MGF and n -th order non-central moment of the SNR γ in the Two-Ray fading model are given, respectively, by

$$\begin{aligned} \phi_\gamma^{(n)}(s) &= \bar{\gamma}^n \exp(\bar{\gamma} s) \sum_{r=0}^n \binom{n}{r} \left(\frac{1}{2}\right)^r \\ &\times \sum_{l=0}^r \binom{r}{l} I_{2l-r}(\bar{\gamma} s), \\ M_\gamma(s) &= \exp(\bar{\gamma} s) I_0(\bar{\gamma} s), \\ \nu_n &= \bar{\gamma}^n \sum_{r=0}^n \binom{n}{r} \left(\frac{1}{2}\right)^r \sum_{l=0}^r \binom{r}{l} \delta_{2l,r}. \end{aligned} \quad (37)$$

Proof: These results are obtained by considering $\xi \rightarrow \infty$ and $\Delta = 1$ in, respectively, (34), (35) and (36). ■

IV. APPLICATIONS TO WIRELESS COMMUNICATION SYSTEMS

The analytical results obtained in the previous sections for the MTW and MTW Extreme fading models are now used

to derive expressions for different performance metrics in wireless communication systems.

A. Outage probability

The channel capacity per unit bandwidth is known to be given by

$$C = \log_2(1 + \gamma). \quad (38)$$

The outage probability is defined as the probability that C falls below a predefined threshold R_s (rate per unit bandwidth), and is calculated as [15, eq. (31)]

$$P_{\text{out}} = F_\gamma(2^{R_s} - 1), \quad (39)$$

where $F_\gamma(\cdot)$ is given in (18) and (31) for the MTW and MTW Extreme fading models, respectively. Note that when the order of the Marcum-Q function is an integer in (18), its numerical computation is much easier since in this case this function is built-in in the main computational software packages.

B. Outage probability in interference-limited scenarios

We now evaluate the outage probability (OP) in an interference-limited scenario, considering an N -branch Maximal Ratio Combining (MRC) receiver and L interfering signals with the same average power P_I . The received signal-to-interference ratio (SIR) can be written as $SIR = \frac{X}{Y}$, where, assuming that the interferers undergo Rayleigh fading, X is the sum of N independent random variables modeling the combiner output signal from the transmitter and Y is the sum of L independent exponential random variables with equal powers modeling the total interference power. The OP is defined as the probability that the SIR falls below a given threshold β , and can be calculated in terms of the generalized MGF of the desired signal as [16, eq. (15)]

$$P_o = \sum_{k=0}^{L-1} \frac{1}{(\beta P_I)^k} \sum_{\Omega_A} \prod_{n=1}^N \frac{1}{q_n!} \phi_{\gamma_n}^{(q_n)}(s) \Big|_{s=-\frac{1}{\beta P_I}}, \quad (40)$$

where γ_n represents in this case the received power of the desired signal at antenna n affected by MTW fading and Ω_A is the set of N -tuples such that $\Omega_A = \{(q_1, \dots, q_N) : q_n \in \mathbb{N}, \sum_{n=1}^N q_n = k\}$. Thus, by using the GMGF given in (22), (34) or (37) for the MTW, MTW Extreme and Two-Ray fading models, respectively, the outage probability under interference is obtained in closed-form. Note that $\bar{\gamma}$ in the computation of the GMGF represents in this case the average power per receive antenna, i.e., we identify $\bar{\gamma} = \bar{W}$.

C. Average energy detection probability

The average probability of energy detection \bar{P}_d of an unknown deterministic signal in the presence of noise in a wireless fading channel can be calculated as [17]

$$\bar{P}_d = \int_0^\infty Q_u\left(\sqrt{2\gamma}, \sqrt{\eta}\right) f_\gamma(\gamma) d\gamma, \quad (41)$$

where $u = TW$, representing the the number of samples obtained in the energy detection, is the product of the one-side bandwidth W and the observation time interval T , which can be easily adjusted to get $u \in \mathbb{N}$, and η is the energy detection threshold. Leveraging the approach in [18], the average detection probability can be given in terms of the generalized MGF as

$$\bar{P}_d = \sum_{n=0}^{\infty} \sum_{q=0}^{u+n-1} \left(\frac{\eta}{2}\right)^q \frac{e^{-\eta/2}}{n!q!} \phi_{\gamma}^{(n)}(s) \Big|_{s=-1}. \quad (42)$$

The average detection probability of an energy detector in MTW fading can be obtained by plugging (22) or (34) into (42), for the general and the extreme cases, respectively. The so-called receiver operating characteristic (ROC) curve is obtained by representing \bar{P}_d vs. P_f , for different values of u and η , where P_f is the false alarm probability, which is given by

$$P_f = e^{-\eta/2} \sum_{k=0}^{u-1} \frac{(\eta/2)^k}{k!}, \quad (43)$$

that is, the detection, in the absence of signal, of noise which is erroneously considered to be signal. On the other hand, a complementary ROC curve is obtained by representing $\bar{P}_m = 1 - \bar{P}_d$, defined as the probability of missed detection (i.e., failing to detect a signal which is present in the channel) vs. P_f .

A useful method to evaluate and compare the system performance for energy detection is the area under the ROC curve (AUC) [19]. The average AUC can be expressed in terms of the generalized MGF as [20, (eq. 13)]

$$\bar{A} = 1 - \sum_{q=0}^{u-1} \sum_{n=0}^q \binom{q+u-1}{q-n} \left(\frac{1}{2}\right)^{n+q+u} \frac{1}{n!} \phi_{\gamma}^{(n)}(s) \Big|_{s=-\frac{1}{2}}, \quad (44)$$

thus obtaining the average AUC for MTW fading by plugging the GMGF in (22) or (34), depending on the case, into (44). These results can be extended to include multiple receive antennas performing MRC diversity for non-coherent energy detectors. In this case, if N is the number of antennas, the instantaneous combined SNR is given by $\gamma = \sum_{k=1}^N \gamma_k$, where γ_k is the instantaneous SNR at the k branch. Assuming that the receive signals at every branch are independent, with the help of the multinomial theorem we can write

$$\phi_{\gamma}^{(n)}(s) = \sum_{\tau(n,N)} \frac{n!}{q_1!q_2!\dots q_N!} \phi_{\gamma_1}^{(q_1)}(s) \dots \phi_{\gamma_N}^{(q_N)}(s), \quad (45)$$

where $\tau(n, N)$ is defined as the set of N -tuples such that $\tau(k, N) = \left\{ (q_1, q_2, \dots, q_N) : q_m \in \mathbb{N}, \sum_{m=1}^N q_m = k \right\}$. Thus, introducing (45) into (42) and (44) together with the GMGF expressions in (22) or (34), depending on the case, the performance of the energy detector for MRC diversity in MTW fading is obtained.

D. Composite IG/MTW Fading Model

We now show that the presented statistical characterization of the MTW and MTW Extreme fading models can be used to

further extend these wireless models to incorporate shadowing. In particular, we consider the effect of shadowing to be modeled by the Inverse Gamma (IG) distribution, which has been shown in [8], thorough empirical validation, to yield a good fit to data measurements, particularly in the cases of mild and moderate shadowing conditions. The received power when IG shadowing and multipath fading are simultaneously considered will be written as

$$Q = \bar{Q}\mathcal{G}\mathcal{V}, \quad (46)$$

where $\bar{Q} = \mathbb{E}\{Q\}$, and \mathcal{G} and \mathcal{V} are independent RVs with normalized power. \mathcal{G} is an IG random variable with shape parameter λ representing shadowing, and \mathcal{V} represents an MTW (or MTW Extreme) fading with $\bar{\gamma} = 1$ (note that γ represents power in this case). We now show that the PDF, CDF, and outage probability of the composite IG/MTW channel model can be obtained in closed-form.

Using the closed-form GMGF in (22) or (34), depending on the considered fading case (MTW or MTW Extreme), together with [8, eq. 12], the PDF of the received power Q is obtained as

$$f_Q(q) = \frac{\bar{Q}^{\lambda}(\lambda-1)^{\lambda}}{q^{\lambda+1}\Gamma(\lambda)} \phi_{\gamma}^{(\lambda)}(s) \Big|_{s=\frac{(1-\lambda)\bar{Q}}{q}}, \quad (47)$$

and the CDF of Q for integer λ is expressed as

$$F_Q(q) = \sum_{n=0}^{\lambda-1} \frac{\bar{Q}^n(\lambda-1)^n}{q^n\Gamma(n+1)} \phi_{\gamma}^{(n)}(s) \Big|_{s=\frac{(1-\lambda)\bar{Q}}{q}}. \quad (48)$$

Besides, the outage probability is given by [21]

$$\begin{aligned} P_{\text{out}}^{\text{IG/MTW}}(\gamma_{th}) &\triangleq P(\gamma_Q < \gamma_{th}) \\ &= F_{\gamma_Q}(\gamma_{th}) \\ &= F_Q\left(\frac{\bar{Q} \times \gamma_{th}}{\bar{\gamma}_Q}\right), \end{aligned} \quad (49)$$

where $\gamma_Q = q\bar{\gamma}_Q/\bar{Q}$ is the SNR at the receiver, $\bar{\gamma}_Q = \mathbb{E}\{\gamma_Q\}$, γ_{th} is the SNR threshold for reliable communication, and $F_Q(q)$ is the CDF given in (48).

V. NUMERICAL RESULTS

Numerical results are now presented for the proposed fading models using the derived expressions in the previous sections, including the representation of the PDF and CDF of the SNR. Different performance metrics under MTW and MTW Extreme fading are computed and verified by simulations, including the outage probabilities in noise-limited and interference-limited scenarios and the average energy detection probability. Also, the outage probability for the composite IG/MTW model, including the extreme case is provided. The distribution parameters are $\{K, \Delta, \mu\}$ for the general model, and $\{\Delta, m\}$ for the extreme model. In the following figures we can observe the influence of these parameters.

In Figs. 1 and 2, the PDF and CDF, respectively, of the MTW fading model are plotted for different values of μ , including the case $\mu = 1$, which corresponds to the TWDP fading model. The numerical results obtained from (17) and (18) are verified by Monte-Carlo simulations, showing an

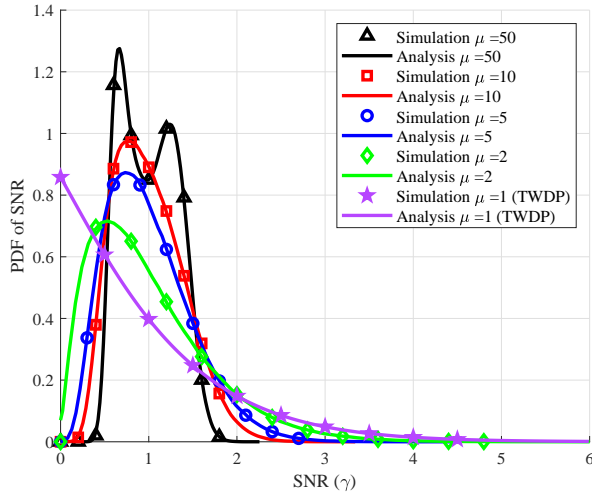


Figure 1. Analysis and simulation results for the PDF of SNR under the MTW fading model with parameters $K = 1$, $\bar{\gamma} = 1$, $\Delta = 0.8$ and different values of $\mu = 2, 5, 10, 50$.

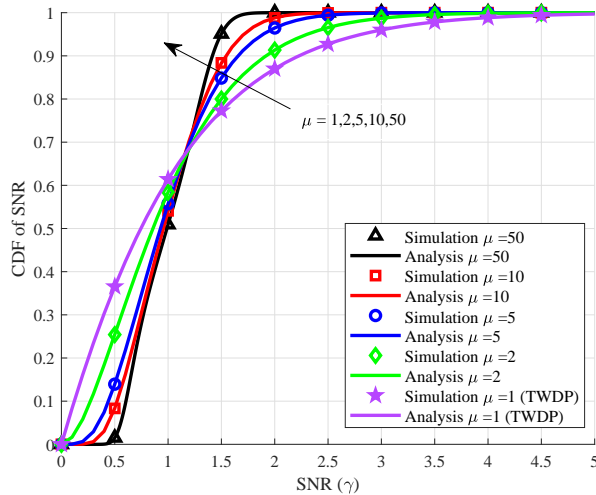


Figure 2. Analysis and simulation results for the CDF of SNR under the MTW fading model with parameters $K = 1$, $\bar{\gamma} = 1$, $\Delta = 0.8$ and different values of $\mu = 2, 5, 10, 50$.

excellent match. It is clear from Fig. 1 that parameter μ has a relevant impact on the shape of the probability distribution, even to the point that, for high values of this parameter ($\mu = 50$) the distribution shows a bimodal behavior, i.e., two local maxima appear in the PDF, while for lower values ($\mu = 2, 5, 10$) only one local (and therefore global) maximum appears. It is also interesting to note that, for the selected parameter values, the case $\mu = 1$, i.e., TWDP fading, yields a monotonic decreasing PDF, with a maximum at the origin. In the CDF curves depicted in Fig. 2, the bimodal behavior is manifested in the appearance of multiple inflection points, which do not appear for the TWDP case ($\mu = 1$) for the selected parameters values. Therefore, parameter μ alone gives the model a great flexibility to fit to different propagation conditions.

In Fig. 3, the PDF (solid lines) and CDF (dashed lines) of

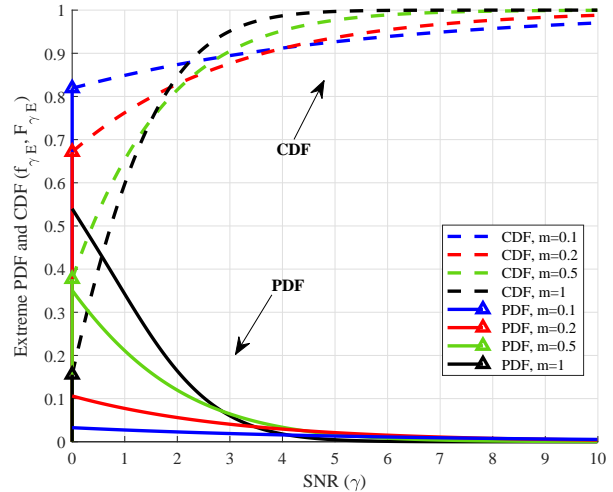


Figure 3. PDF and CDF of the MTW Extreme fading for different $m = 0.1, 0.2, 0.5, 1$, and with parameters $\bar{\gamma} = 2$ and $\Delta = 0.8$.

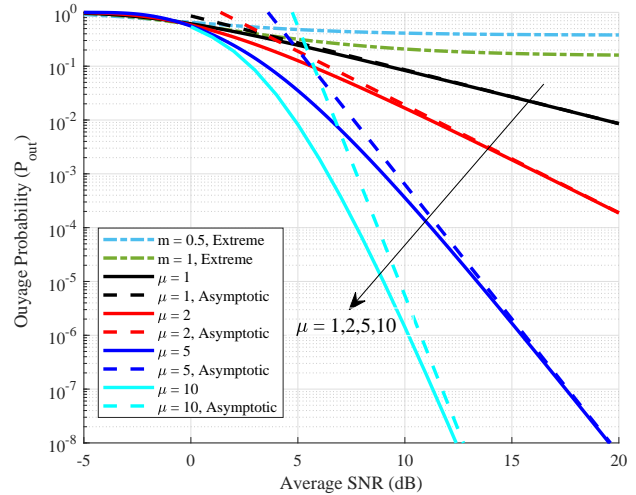


Figure 4. Outage probability P_{out} vs. average SNR for MTW fading, asymptotic behavior in high SNR and the extreme case considering different number of clusters ($\mu = 1, 2, 5, 10$) and $m = 0.5, 1$ for the extreme case, and parameters $K = 1$, $\Delta = 0.8$, and $R_s = 1$.

the MTW Extreme fading model, which is analyzed in Section III, are presented for different values of m . A remarkable fact in this case is the appearance of the Dirac delta function in the PDF, as justified in the theoretical analysis. This is useful to model field-realistic measurements, as it captures the fact that no signal is received at all ($\gamma = 0$) with a non-zero probability. Therefore, the corresponding CDF has the same value at the origin as the weight factor of the Dirac delta function in the PDF. It can be observed that the higher the value of m the lower the probability of no signal reception. This is a result of m being equal to $1/\text{AoF}$, i.e., the higher the value of m the lower the channel variations.

Figs. 4 and 5 present the outage probability without interference and considering the interference effect, respectively. Fig. 4 shows the outage probability vs. average SNR under

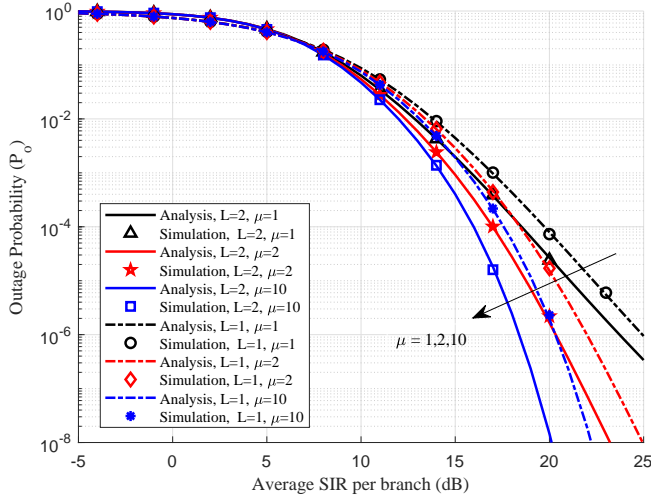


Figure 5. Outage probability P_o vs. average SIR per branch according to (40) for MTW fading considering different number of clusters ($\mu = 1, 2, 10$) and interferers ($L = 1, 2$), and parameters $K = 10$, $\Delta = 0.8$, $N = 3$, and $\beta = 10$.

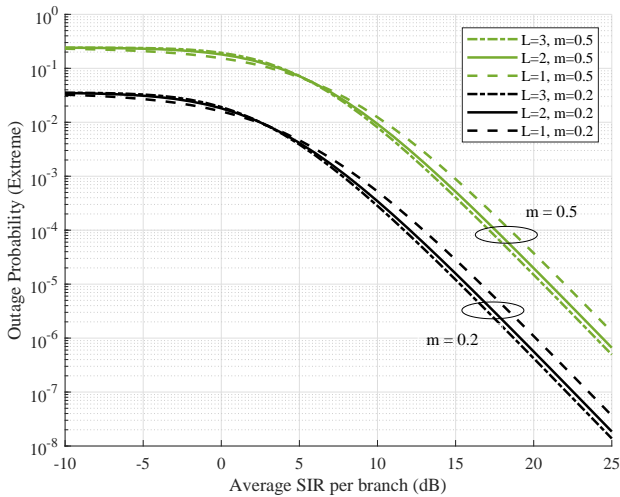


Figure 6. Outage probability P_o vs. average SIR per branch according to (40) for MTW Extreme fading considering different fading severity ($m = 0.2, 0.5$) and number of interferers ($L = 1, 2, 3$), and parameters $\Delta = 0.8$, $N = 3$, and $\beta = 10$.

MTW fading, and the asymptotic behavior and the extreme case are also shown considering different numbers of clusters $\mu = 1, 2, 5, 10$, and fading severity parameter $m = 0.5, 1$ for the extreme case. It be observed that the outage probability decreases by raising the number of clusters μ in the general case and the fading parameter m in the extreme case. The asymptotic curves clearly show the effect of the diversity order (higher slope in the high SNR regime as μ increases). It is worth noting that the diversity order in the extreme case is zero, and therefore the outage probability tends to a constant value in the high SNR regime. Fig. 5 depicts the outage probability vs. the average SIR per branch, $\bar{W}/(L \cdot P_I)$, in an interference-limited scenario with N branch MRC under MTW fading and L interferers experiencing Rayleigh fading

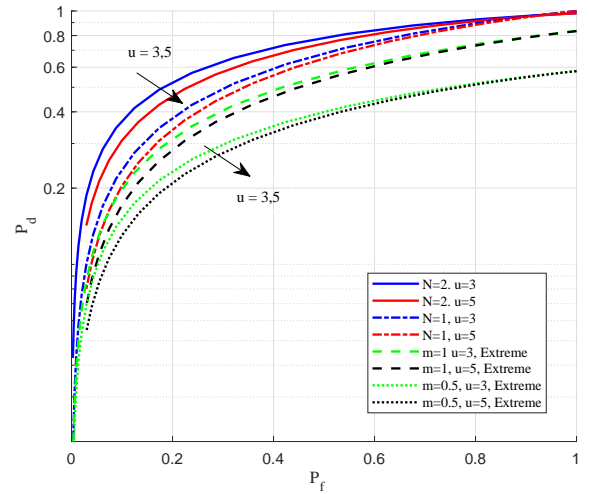


Figure 7. ROC curve (average \bar{P}_d vs. average P_f) under MTW fading for different numbers of receive diversity branches N and number of samples u , when $K = 10$ and $\mu = 5$. MTW Extreme fading results are also given for different fading severity m and u . $\Delta = 0.3$ and $\bar{\gamma} = 1$.

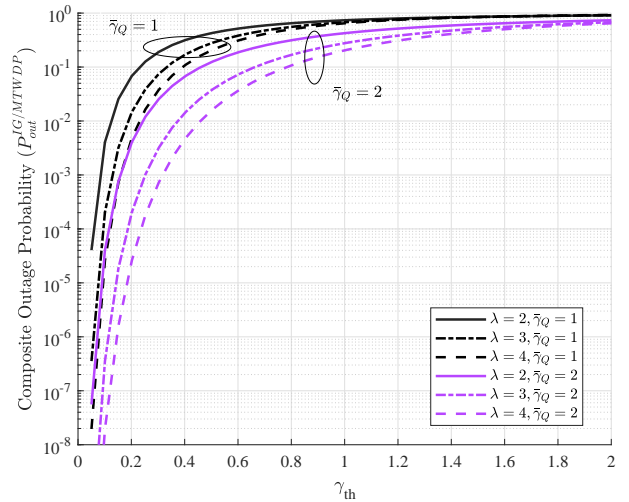


Figure 8. Outage probability of the composite IG/MTW model vs. SNR threshold (γ_{th}) with parameters $\mu = 5$, $K = 10$, $\Delta = 0.3$, $\bar{\gamma} = 1$, and $\bar{Q} = 1$.

with equal average power P_I . The figure shows analytical results, obtained using (40), which are verified by Monte-Carlo simulations, considering parameter values $\mu = 1, 2, 10$ and $L = 1, 2$. It can be observed that parameter μ of the MTW channel model has a significant impact on the outage probability, especially for high average SIR. It can also be seen that the outage probability decreases by increasing μ , i.e., it is more beneficial that the signal power is distributed among different clusters. Also, increasing the number of interferers raises the probability of outage, and the system performance worsens, which could be compensated by exploiting the MRC technique by increasing the number of antennas at the receiver.

Fig. 6 shows the outage probability for the MTW Extreme fading under interference, where the impact of parameters

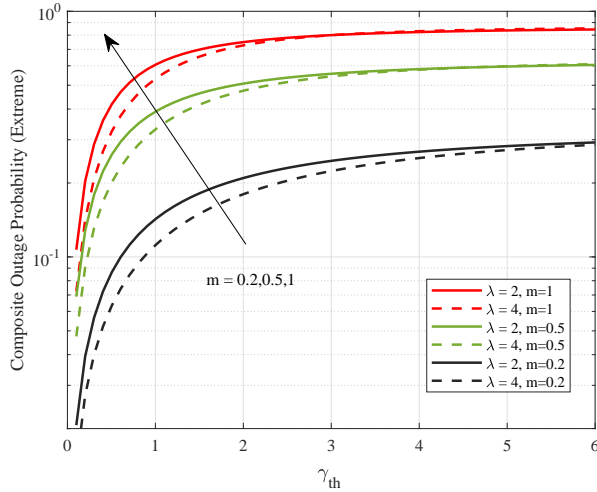


Figure 9. Outage probability of the composite IG/MTW Extreme model vs. SNR threshold (γ_{th}) with parameters $\Delta = 0.3$, $\bar{\gamma} = 1$, $\bar{\gamma}_Q = 1$ and $\bar{Q} = 1$.

L and m on performance is depicted. Raising the number of interferers increases the outage probability, and higher m , which represents lower severity fading and therefore less channel variations, increases the outage probability for the considered parameters values, as a result of a lower probability that the desired signal is received with high power.

Fig. 7 presents ROC curves (\bar{P}_d vs. P_f) to analyze the effect on an energy detector of parameter u (number of samples) and the number of receive antennas at the MRC receiver when the channel undergoes MTW fading. The average probability of energy detection (\bar{P}_d) and false alarm probability (P_f) are given in (42) and (43), respectively. It can be observed that the ROC curves rise noticeably when the number of MRC branches increases and, for a given number of branches in the MRC receiver, lower u shows a better result. Thus, increasing the number of samples u decreases the AUC for a given SNR per branch. ROC curves are also shown in this figure when the channel undergoes MTW Extreme fading for different values of parameters m and u . Again, decreasing u yields a better result, while increasing m (less severe fading) yields an increase in the energy detection probability.

Finally, Fig. 8 presents numerical results of the outage probability for the IG/MTW channel model, while Fig. 9 shows results for the extreme case. The outage probability in (49) is plotted as a function of the SNR threshold for different values of the IG parameter $\lambda = 2, 3, 4$ and for average SNR $\bar{\gamma}_Q = 1, 2$. As expected, the outage probability increases by rising the SNR threshold and, for a given threshold, increasing the average SNR reduces the outage probability. Also, low γ_{th} and high values of the shape parameter of the IG distribution λ yields a lower outage probability. The composite outage probability for the extreme case is plotted for different values of the IG parameter $\lambda = 2, 4$ and the fading severity parameter $m = 0.2, 0.5, 1$ in Fig. 9. It can be seen that the shape parameter λ yields a similar behavior in the extreme case as for the general. Also, rising m increases the outage probability for the selected parameter values.

VI. CONCLUSIONS

We have presented the Multi-cluster Two-Wave fading model, by defining its physical model and deriving its chief probability functions. The unique features of the MTW model allow to simultaneously control both the diversity order and the distribution bimodality, encompassing the well-established κ - μ and TWDP fading models as special cases. Special attention has been paid to the extreme behavior of the MTW fading model, providing additional compact expressions for all the statistics functions describing the model. The derived expressions for the MTW and MTW Extreme models, which are given in closed-form for the case of Laplace-domain statistics, and in simple finite-range integral form for the PDF and CDF, can be directly applied for performance analysis purposes and have been consequently exemplified.

The MTW fading model can be further extended to include fluctuations of the specular components [22], thus connecting with the popular Fluctuating Two-Ray (FTR) and κ - μ shadowed fading models [15], [23]. However, we note that the formulation in [22] only connects with the MTW fading in a limit case by letting one of the parameters grow to infinity, while the derivations here presented have compact form and a reduced number of parameters.

APPENDIX A PROOF OF LEMMA 2

To prove Lemma 2, we first introduce (17) into (21), yielding

$$\begin{aligned} \phi_{\gamma}^{(n)}(s) &= \frac{\mu}{\pi} \left(\frac{1+K}{\bar{\gamma}} \right)^{\frac{\mu+1}{2}} \left(\frac{1}{K} \right)^{\frac{\mu-1}{2}} e^{-\mu K} \\ &\times \int_0^{\pi} e^{-\mu K \Delta \cos \theta} (1 + \Delta \cos \theta)^{\frac{1-\mu}{2}} \\ &\times \left[\int_0^{\infty} x^{n+\frac{\mu-1}{2}} e^{-x(\mu\frac{1+K}{\bar{\gamma}}-s)} \right. \\ &\times \left. I_{\mu-1} \left(2\mu \sqrt{\frac{1+K}{\bar{\gamma}} K (1 + \Delta \cos \theta) \sqrt{x}} \right) dx \right] d\theta. \end{aligned} \quad (50)$$

The inner integral in (50) is a Laplace transform that can be solved, with the help [24, (3.15.2.9)], as

$$\begin{aligned} \mathfrak{L} \{ x^{n+\frac{\nu}{2}} I_{\nu} (a\sqrt{x}) ; z \} \\ = \left(\frac{a}{2} \right)^{\nu} n! z^{-\nu-n-1} e^{\frac{a^2}{4z}} L_n^{\nu} \left(\frac{-a^2}{4z} \right), \end{aligned} \quad (51)$$

where $\Re(\nu) > -n-1$, $\Re(z) > 0$, $|\arg(a)| < \pi$ and $L_n^{\nu}(\cdot)$ is the generalized Laguerre function [25, (22.3.9)]

$$\begin{aligned} L_n^{\nu}(z) &= \sum_{q=0}^n (-1)^q \binom{n+\nu}{n-q} \frac{z^q}{q!} \\ &= \sum_{q=0}^n (-1)^q \frac{\Gamma(\nu+n+1)z^q}{\Gamma(\nu+q+1)(n-q)!q!}. \end{aligned} \quad (52)$$

After substitution, developing the binomial with $\Delta \cos \theta$ and some manipulations, we obtain

$$\begin{aligned} \phi_{\gamma}^{(n)}(s) &= \frac{\Gamma(\mu+n)}{\pi} \exp\left(\frac{s\mu K}{\mu\frac{1+K}{\gamma}-s}\right) \\ &\times \sum_{q=0}^n \binom{n}{q} \frac{\mu^{\mu+2q}}{\Gamma(\mu+q)} \left(\frac{1+K}{\gamma}\right)^{\mu+q} \\ &\times K^q \left(\mu\frac{1+K}{\gamma}-s\right)^{-\mu-n-q} \sum_{m=0}^q \binom{q}{m} \Delta^m \\ &\times \int_0^{\pi} (\cos \theta)^m \exp\left(\frac{s\mu K \Delta}{\mu\frac{1+K}{\gamma}-s} \cos \theta\right) d\theta. \end{aligned} \quad (53)$$

With the help of [26, eq. (14)], the integral in (53) can be solved in closed-form as

$$\begin{aligned} I &= \int_0^{\pi} (\cos \theta)^m \exp(\alpha \cos \theta) d\theta \\ &= \pi \frac{1}{2^m} \sum_{l=0}^m \binom{m}{l} I_{2l-m}(\alpha) \end{aligned} \quad (54)$$

where $\alpha = \frac{\mu K \Delta s}{\mu\frac{1+K}{\gamma}-s}$. Then, by introducing (54) into (53), (22) is obtained.

REFERENCES

- [1] M. Olyaei, J. P. Peña-Martín, F. J. Lopez-Martinez, and J. M. Romero-Jerez, "Statistical characterization of the multicluster two-wave fading model," in *Proc. 2022 5th International Conference on Advanced Communication Technologies and Networking (CommNet)*, 2022.
- [2] M. D. Yacoub, "The $\kappa - \mu$ distribution: a general fading distribution," in *IEEE 54th Vehicular Technology Conference. VTC Fall 2001. Proceedings (Cat. No.01CH37211)*, vol. 3, 2001, pp. 1427–1431.
- [3] M. Yacoub, "The $\kappa - \mu$ distribution and the $\eta - \mu$ distribution," *IEEE Antennas Propag. Mag.*, vol. 49, no. 1, pp. 68–81, Feb. 2007.
- [4] G. Durgin, T. Rappaport, and D. A. de Wolf, "New analytical models and probability density functions for fading in wireless communications," *IEEE Trans. Commun.*, vol. 50, no. 6, pp. 1005–1015, Jun. 2002.
- [5] J. Frolik, "A case for considering hyper-rayleigh fading channels," *IEEE Trans. Wireless Commun.*, vol. 6, no. 4, pp. 1235–1239, Apr. 2007.
- [6] E. Zöchmann, S. Caban, C. F. Mecklenbräuker, S. Pratschner, M. Lerch, S. Schwarz, and M. Rupp, "Better than Rician: modelling millimetre-wave channels as two-wave with diffuse power," *EURASIP Journal on Wireless Communications and Networking*, vol. 2019:21, pp. 1–17, 2019.
- [7] G. S. Rabelo and M. D. Yacoub, "The $\kappa - \mu$ extreme distribution," *IEEE Trans. Commun.*, vol. 59, no. 10, pp. 2776–2785, Oct. 2011.
- [8] P. Ramírez-Espinosa and F. J. Lopez-Martinez, "Composite fading models based on inverse gamma shadowing: Theory and validation," *IEEE Trans. Wireless Commun.*, vol. 20, no. 8, pp. 5034–5045, 2021.
- [9] M. Rao, F. Lopez-Martinez, M. Alouini, and A. Goldsmith, "MGF approach to the analysis of generalized two-ray fading models," *IEEE Trans. Wireless Commun.*, vol. 14, no. 5, pp. 2548–2561, May 2015.
- [10] M. K. Simon and M.-S. Alouini, *Digital Communications over Fading Channels*, 2nd ed. John Wiley & Sons, Inc., 2005.
- [11] J. P. Peña Martín, J. M. Romero-Jerez, and F. J. Lopez-Martinez, "Generalized MGF of Beckmann fading with applications to wireless communications performance analysis," *IEEE Trans. Commun.*, vol. 65, no. 9, pp. 3933–3943, Sep. 2017.
- [12] U. Charash, "Reception through Nakagami fading multipath channels with random delays," *IEEE Trans. Commun.*, vol. COM-27, no. 4, pp. 657–670, Apr. 1979.
- [13] Z. Wang and G. Giannakis, "A simple and general parameterization quantifying performance in fading channels," *IEEE Trans. Commun.*, vol. 51, no. 8, pp. 1389–1398, Aug. 2003.
- [14] J. M. Romero-Jerez, F. J. Lopez-Martinez, J. P. Peña-Martín, and A. Abdi, "Stochastic fading channel models with multiple dominant specular components," *IEEE Trans. Veh. Technol.*, vol. 71, no. 3, pp. 2229–2239, 2022.
- [15] J. M. Romero-Jerez, F. J. Lopez-Martinez, J. F. Paris, and A. J. Goldsmith, "The fluctuating two-ray fading model: Statistical characterization and performance analysis," *IEEE Trans. Wireless Commun.*, vol. 16, no. 7, pp. 4420–4432, Jul. 2017.
- [16] J. M. Romero-Jerez and A. J. Goldsmith, "Receive antenna array strategies in fading and interference: an outage probability comparison," *IEEE Trans. Wireless Commun.*, vol. 7, no. 3, pp. 920–932, 2008.
- [17] F. Digham, M.-S. Alouini, and M. K. Simon, "On the energy detection of unknown signals over fading channels," *IEEE Trans. Commun.*, vol. 55, no. 1, pp. 21–24, Jan. 2007.
- [18] A. Annamalai, O. Olabiyyi, S. Alam, O. Odejide, and D. Vaman, "Unified analysis of energy detection of unknown signals over generalized fading channels," in *Wireless Communications and Mobile Computing Conference (IWCMC), 2011 7th International*, Jul. 2011, pp. 636–641.
- [19] S. Atapattu, C. Tellambura, and H. Jiang, "Analysis of area under the ROC curve of energy detection," *IEEE Trans. Wireless Commun.*, vol. 9, no. 3, pp. 1216–1225, Mar. 2010.
- [20] O. Olabiyyi, S. Alam, O. Odejide, and A. Annamalai, "Efficient evaluation of area under the ROC curve of energy detectors over fading channels," in *Proc. ACM/IEEE MSWiM'11*. NY, USA: ACM, 2011, pp. 261–264.
- [21] A. Goldsmith, *Wireless communications*. Cambridge university press, 2005.
- [22] J. D. Vega Sánchez, F. J. López-Martínez, J. F. Paris, and J. M. Romero-Jerez, "The multi-cluster fluctuating two-ray fading model," *arXiv e-prints*, 2022. [Online]. Available: <https://arxiv.org/abs/2212.02448>
- [23] J. Paris, "Statistical characterization of $\kappa - \mu$ shadowed fading," *IEEE Trans. Veh. Technol.*, vol. 63, no. 2, pp. 518–526, Feb. 2014.
- [24] A. P. Prudnikov, Y. A. Brychkov, and O. I. Marichev, *Integrals and Series: Direct Laplace Transforms*. CRC, 1992, vol. 4.
- [25] M. Abramowitz and I. A. Stegun, *Handbook of Mathematical Functions with Formulas, Graphs, and Mathematical Tables*, 10th ed. U.S. Department of Commerce - N.B.S., Dec. 1972.
- [26] N. Y. Ermolova, "Capacity analysis of two-wave with diffuse power fading channels using a mixture of gamma distributions," *IEEE Commun. Lett.*, vol. 20, no. 11, pp. 2245–2248, 2016.